

The most common refrigerant-absorbent pairs used in the absorption cycle are water/lithium bromide ($\text{H}_2\text{O}/\text{LiBr}$) and ammonia/water ($\text{NH}_3/\text{H}_2\text{O}$). Since the $\text{H}_2\text{O}/\text{LiBr}$ system has high volatility ratio, it can operate at low pressures and, therefore, at lower generator temperature. However, the operation of the $\text{H}_2\text{O}/\text{LiBr}$ -based absorption cycle is limited in the evaporating temperature and the absorber temperature, due to the freezing of the water and the solidification of the LiBr -rich solution, respectively. Therefore, they are operated at evaporator temperatures of 5°C or higher [4] and are mostly water cooled. Typical cooling COPs of the single-effect, double-effect, and triple-effect $\text{H}_2\text{O}/\text{LiBr}$ absorption cycles are 0.7, 1.2, and 1.7, respectively [3]. The operation of the $\text{NH}_3/\text{H}_2\text{O}$ -based absorption cycle is not limited in either the evaporating temperature or the absorption temperature. Consequently, the $\text{NH}_3/\text{H}_2\text{O}$ system has the advantage that it can be operated down to very low temperatures. A rectifying column after the boiler is required to remove water vapor from ammonia as much as possible which helps prevent ice crystals from forming for temperature much below 0°C .

There had been many attempts in the Arabian Gulf Countries to utilize solar energy for the purpose of cooling and air conditioning. An integrated solar cooling system utilizing three types of solar subsystems was used to air condition a residential building in Kuwait [5]. The system had been installed and tested in the Kuwait Institute for Scientific Research solar house. The first system was a solar photovoltaic power system which produced 2 kW peak power at 48 V d.c. and used 1200 AH battery storage. The second system was a solar air heating system which consisted mainly of a 60 m^2 collector area (air type) and a 7.2 m^3 rock storage system. The third one was a solar water heating, cooling and domestic water heating system. The solar cooling system used an 11 kW $\text{LiBR}/\text{H}_2\text{O}$ absorption system, a 96 m^2 collector area (water type), 7.5 m^3 hot water storage and 4 m^3 chilled water storage. The author reported that a corrosion problem had occurred in the water collectors which made them unserviceable.

In addition, three 35kW $\text{LiBR}/\text{H}_2\text{O}$ absorption chillers were installed for an office building of the Ministry of Defense in Kuwait [6]. These chillers were water cooled via a roof mounted cooling tower. The system used 300 m^2 of flat plate water collector area and a vertical hot water tank of 20 m^3 . An oil fired water heater of 130 kW capacity was also used.

Beside experimental work, various computer simulation programs had been developed to predict the performance of solar cooling system in nearby countries. In Jeddah, Saudia Arabia, a solar-powered combined system comprising a $\text{LiBR}/\text{H}_2\text{O}$ absorption chiller and a multiple-effect distillator had been theoretically investigated [7]. The multiple-effect distillator was powered by the rejected heat from the absorption machine. Moreover, tracking parabolic troughs oriented in the North-South axis were used to collect solar energy. The overall COP of the system reached 1.44.

The Iraqi solar house cooling system, built in early eighties, was simulated using different computer programs [8]. In order to completely simulate the solar cooling system, a number of computer programs were developed and used simultaneously with TRNSYS program [9]. The total effective collector area was 243 m^2 . 128 flat plate collectors with a single glass cover of 1.89 m^2 area each were oriented at 22.5° East of South with a summer operation tilt angle of 15.6° . The $\text{LiBR}/\text{H}_2\text{O}$ absorption chiller used had a capacity of 35 kW.

There is scarcity on the investigation of solar cooling system in the U.A.E. A few studies have been reported on the subject. A parametric analytical study of a roof solar chimney coupled with wind-cooled cavity for natural ventilation in building was presented for Al-Ain city [10]. The proposed system is capable of creating an air flow rate up to 1.6 kg/s. It had been concluded that the natural air flow cooled cavity was less effective in terms of cooling. The system was reconsidered in order to be resized and improved [11]. ACTION Psychrometrics Software [12] was used to predict the mean cooling load corresponding to the induced air flow rate. It was found that an ACH up to 26 could be achieved, which indicated an increase in the induced air flow rate by the modified chimney by three times.

A solar liquid desiccant system was proposed for greenhouse food production [13]. The idea was to dry the air before entering an evaporative cooler, which lowers the wet-bulb temperature of the air. The system was found to lower the maximum summer temperature by 15°C compared to a simple fan ventilated green house and 5°C lower than the temperature achieved by conventional evaporative cooling system. This effect would lead to extending the optimum season for the vegetables.

Building-integrated solar photovoltaic systems for a hybrid solar cooled ventilation technique was investigated [14]. The main focus of the study was to regulate solar panels maximum power operation and ensure maximum tracking. Two PV interface schemes were presented: PV-Battery-permanent magnet motor drive for air conditioning mechanical unit (1-15 kW) and PV-DC-AC solid-state inverter, driving a three phase induction motor for ventilation and air conditioning loads (15-50 kW).

It has to be noted that solar energy has been utilized in the U.A.E. for other purposes, such as desalination [15, 16], but this study focuses on solar cooling and air conditioning. To the best of the author's knowledge, solar absorption cooling has not been investigated yet for the U.A.E. climate

conditions. In this paper TRNSYS simulation of a solar powered NH₃/H₂O absorption cycle is presented. A parametric study is also carried out to size and optimize the system for best performance.

2. System Description

The solar powered absorption cycle is divided into two sub-systems namely, the solar sub-system and the cooling sub-system. The former includes the solar collector array, a thermally insulated storage tank, an auxiliary heater and two pumps. The cooling sub-system consists mainly of the absorption cycle, a cooling tower, a water-to-air heat exchanger and the space to be conditioned. The schematic of the solar powered absorption system is shown in Figure 2.

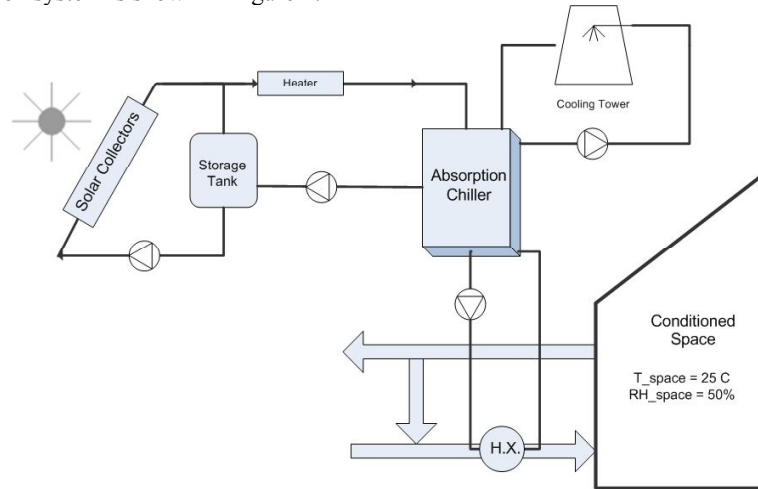


Figure 2. Schematic of the solar absorption air conditioner.

The specifications of the solar collector are based on a commercially available evacuated tube collector ETC [Error! Reference source not found.]. The ETC consists of 30 evacuated tubes with copper heat pipes. The absorber plate is coated with high efficiency selective coating, graded Al-N/Al, $\alpha > 0.92$ and $\epsilon < 0.08$. The absorber plate and the heat pipe are sealed within the evacuated glass tube. The glass used is Borosilicate glass with $\tau \geq 0.91$. The overall heat loss coefficient of the collector is $0.7 \text{ W/m}^2 \cdot ^\circ\text{C}$.

The cooling cycle considered in this study is a single stage water cooled absorption chiller. It is a small scale chiller, 10 kW [17]. The refrigerant/absorbent pair is NH₃/H₂O.

3. System Modeling

Computer modeling of the complete system performance is very important. With such models, the system performance can be predicted for different climate conditions. Various components can also be optimized and sized. Prior modeling of the system is performed to eliminate the expenses associated with building different prototypes. The models can also help estimate the solar collector contribution and the amount of energy required to support the collectors.

The system is modeled with TRNSYS program. It consists of many subroutines, called Types, which model various sub-system components. Once all the components have been selected, these models are linked together to form the system model. TRNSYS solves the set of equations created by the system at each time step. The user has to define the components' parameters and decide on the information transferred from one component to the other. Therefore, it is necessary to construct an information flow diagram for the system once all the components of the system have been identified. The information flow diagram for the whole system is created as shown in Figure 3.

A Typical Meteorological Year 2, TMY2, data file is used to obtain the solar irradiance and various weather conditions for Abu Dhabi. This TMY2 file is based on the global meteorological database [18]. In order to calculate the diffuse irradiance on tilted surfaces, Perez model is selected.

A single ETC collector has an aperture area of 2.79 m^2 . The thermal efficiency of the ETC is based on aperture area and mean temperature:

$$\eta_{th} = a_o - a_1 \frac{(\Delta T_{avg})}{G} - a_2 \frac{(\Delta T_{avg})^2}{G} \quad (1)$$

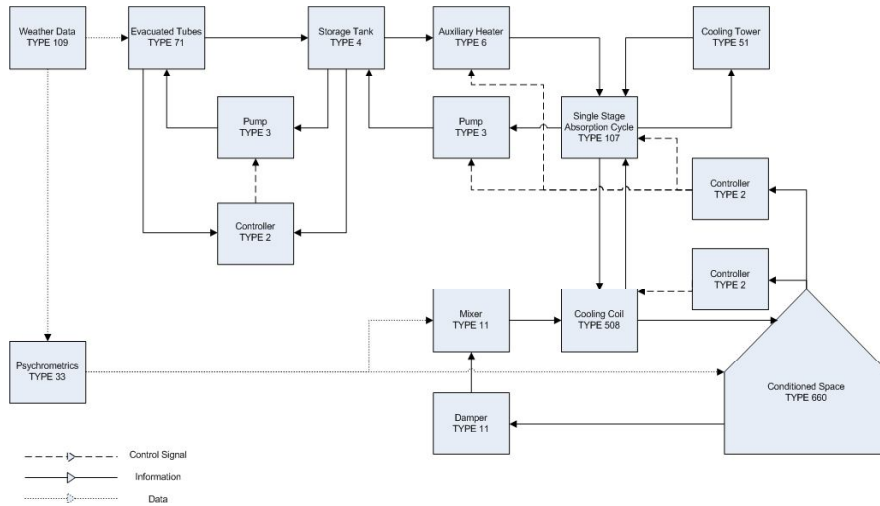


Figure 3. System information flow diagram.

The characteristics of the ETC used in the TRNSYS simulations can be found in Table 1.

ETCs are optically non-symmetric, so biaxial incidence angle modifiers are provided in an external data file. The collector test reports the transversal K_T and longitudinal K_L incidence angle modifiers as shown in Table 2. The K_L is measured in a plane that is perpendicular to the collector plane and contains the collector azimuth, whereas K_T is measured in a plane that is perpendicular to both the collector aperture and the longitudinal plane.

The technical data of the absorption chiller as reported by the manufacturer can be found in

Table 3.

The COP of chiller is defined based on Equation **Error! Reference source not found.**)

$$COP = \frac{Q_{evap}}{Q_{gen} + P_{elec}} \quad (2)$$

The cooling tower is sized based on the 2% evaporation design conditions for Abu Dhabi with a wet bulb temperature of 29.2°C and mean coincident dry bulb temperature of 34.1°C [19]. McQuiston et al. listed performance data for few factory assembled cooling towers ranging from 176-2110 kW [21]. These data are extrapolated to obtain the performance of a suitable cooling tower for the small scale absorption chiller.

A brief description of the other key components can be found in Table 4.

Differential controllers are implemented to simulate real world situations. The collector pump controller turns the pump ON or OFF based on the working fluid temperature increase across the collector array. Once the temperature of the collector exceeds the temperature at the bottom of the storage tank by 5-10K, the collector pump is turned ON. Whereas if the temperature at the collector output is lower than that of the input by 2K, the pump is turned OFF [22]. More strict temperature variation has been reported in the literature where the ON/OFF controller for circulating pump is actuated when the temperature difference across collector array exceeded 3K and stopped when this difference is less than 0.5K [8].

In addition, controlling the absorption chiller, auxiliary heater and the load pump is based on the zone conditions. They are activated when the temperature inside the conditioned space increases by 3K above the setting temperature, 20°C, and deactivated when the temperature drops by 2K below the setting temperature. Moreover, the cooling coil is bypassed according to the previous control scheme.

Table 1. ETC characteristics.

Parameter	Value
Efficiency mode	2
Flow rate at test conditions	70 kg/hr.m ²
a ₀	0.734
a ₁	1.529 W/m ² .K
a ₂	0.0166 W/m ² .K ²

Table 2. Incidence angle modifiers.

θ_i [°]	0	10	20	30	40	50	53	60	70	80	90
K_T	1.00	1.00	1.03	1.11	1.25	1.37	1.40	1.36	1.11	0.70	0.05
K_L	1.00	1.00	1.00	0.99	0.96	0.92	0.88	0.84	0.69	0.44	0.00

Table 3. Absorption cycle technical data.

Heat Exchanger Capacity [kW]		Mass Flow Rate [kg/hr]	
Evaporator	10.0	Chilled Water	1,437
Condenser and Absorber	28.2	Cooling Water	4,859
Generator	18.2	Heating Water	2,239
Temperature [°C]		Electrical Input	
Chilled Water	In = 12 Out = 6	Power	400W
Cooling Water	In = 24 Out = 29	Voltage	600 V/3 Ph, 60 Hz
Heating Water	In = 85 Out = 78		

Table 4. Parameters of components used in TRNSYS simulation.

Component	Parameter	Value
Simple lumped capacitance multi-zone building model	UA	1000 kJ/hr.K
	Capacitance of Zone	24000 kJ/K
	Volume	250 m ³
	T_{init}	30°C
	W_{init}	0.01 kg _w /kg _a
Sensible energy storage tank subject to thermal stratification having user defined inlet positions	Infiltration flow rate	75 kg/hr
	Fluid specific heat	4.19 kJ/ kg.K
	Fluid density	1000 kg/m ³
	Tank loss coefficient	3 kJ/hr.m ² .K
	Number of nodes	10
	Height of each node	0.05 m
	Boiling point	100°C
	Entering node for hot-source flow	1
Entering node for cold-side fluid	1	

4. System Optimization

The performance of the system is affected by various factors. The factors considered in this study are the collector tilt angle, the mass flow rate through the collectors, the heater setting temperature, the storage tank volume and the collector area. A number of runs were carried out in order to optimize these factors. Each run represents one year simulation.

The effect of the collector tilt angle for a south facing collector has been investigated. The latitude and longitude values of the Abu Dhabi are 24.43°N and 54.45°E, respectively. It is known that the highest and lowest values of solar altitude are simply the value of the local latitude $\pm 23.5^\circ$. Therefore, different values of collector tilt angles with an increment of 12° from the horizontal position are used, as shown Figure 4. Moreover, the initial configuration of the solar subsystem consists of a 1 m³ hot water storage tank, a mass

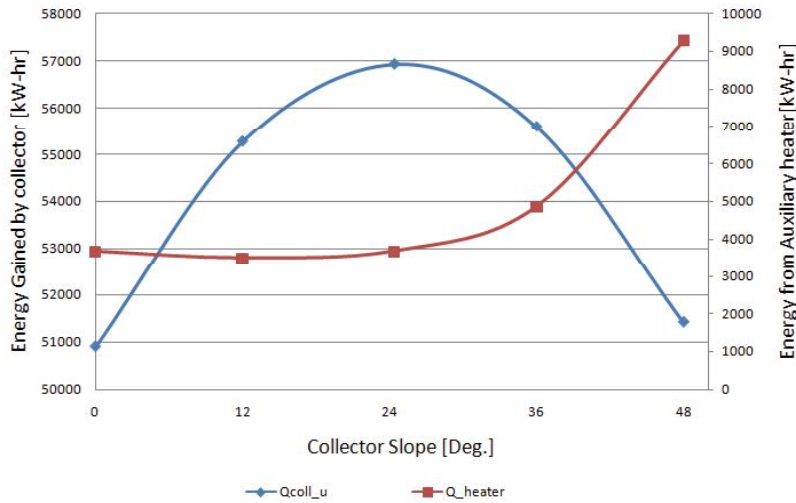


Figure 4. Effect of collector's slope angle.

flow rate through the collectors array of 400 kg/hr and a boiler thermostat setting of 85°C. The initial size of the collector area is chosen to be 70 m². According to SACE evaluation report, the average specific collector for NH₃/H₂O absorption cycles is 7.2 m² per 1 kW of cooling for capacities ranging from 5 to 12 kW [23].

The results from Figure 4 show that the highest seasonal collector energy gain is when the slope angle is equal to the local latitude. The results also show that the amount of energy provided by the auxiliary heater increases for tilt angles higher than the 24.4° even though the collector energy gain is very close to that of lower tilt angles. The reason is that a large percentage of the gained heat by the collectors is not during the summer season when cooling is most needed. In order to increase the solar fraction SF, Equation (2), minimizing the auxiliary heater energy is desirable.

$$SF = \frac{Q_{coll_u}}{Q_{gen}} = 1 - \frac{Q_{heater}}{Q_{gen}} \quad (2)$$

The effect of varying the mass flow rate through the collector array is investigated. Figure 5 shows the amount of energy gained by the collector and the amount of energy provided by the auxiliary heater integrated over one year period. It can be clearly seen that as the mass flow rate increases, the heater energy reduces while the collector heat gain increases. The reduction in the auxiliary heater energy is sharp between 100-200 kg/hr and starts approaching flat for higher values.

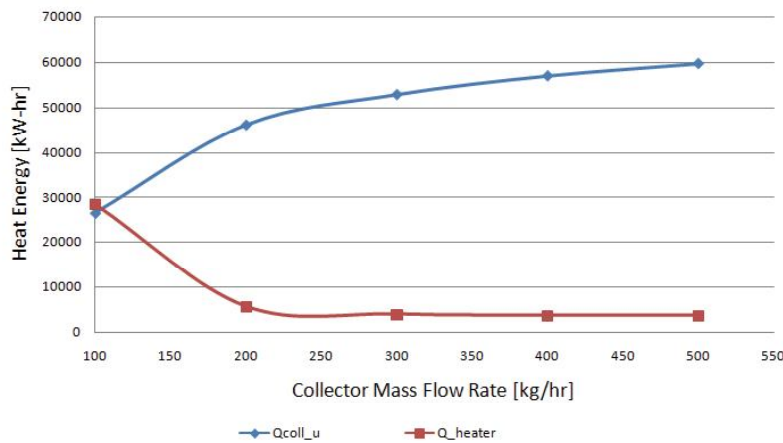


Figure 5. Collector mass flow rate vs. gained and provided heat energy.

In order to meet the required absorption driving temperature, an auxiliary heater is put in series with the storage tank. This configuration is found to consume less energy. A heater thermostat is used to control its operation, allowing the heater to operate only when the temperature of the fluid delivered to the absorption cycle is below the required value. The results of changing the heater setting temperature are shown in Figure 6. Intuitively, increasing the thermostat setting temperature would lead to increase the heater energy requirements. The figure shows that there is a reduction in the collector heat gain since the collector fluid inlet temperature increases with increasing the setting temperature. However, this reduction is considered small compared to flat plate solar collectors since ETCs are designed to operate with high efficiency at high temperatures.

The fact that the returning hot water temperature from the absorption cycle to the storage tank could be higher than the temperature of the water leaving it has been taken into consideration. A stratified storage tank with its both inlets located at the top is modeled. An optimum storage tank size exists and it can be found by examining the influence of storage size on the system performance as shown in Figure 7. It can be seen that smaller hot water storage tanks are not able to store enough energy which increases the load on the heater. It can also be concluded that there is no benefits of increasing the hot water storage tank size above 1 m³.

The results of varying the collector area on the collector gained energy and the required auxiliary heater energy can be seen in Figure 8. The purpose of the solar sub-system is to insure that most of the absorption cycle required heat is provided by the collectors otherwise the system would be unfeasible. The figure shows that the required heater energy reduces and the collectors' useful heat increases, as expected. It can be seen that smaller savings on heater power would be obtained if the area increases more than 60 m².

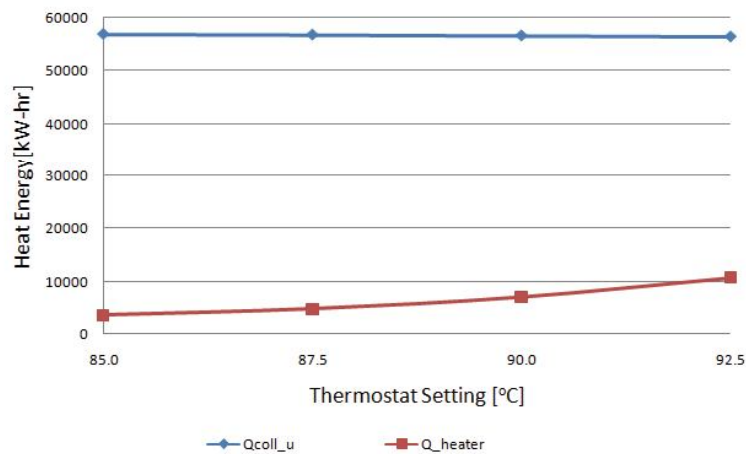


Figure 6. The effect of changing the heater setting temperature.

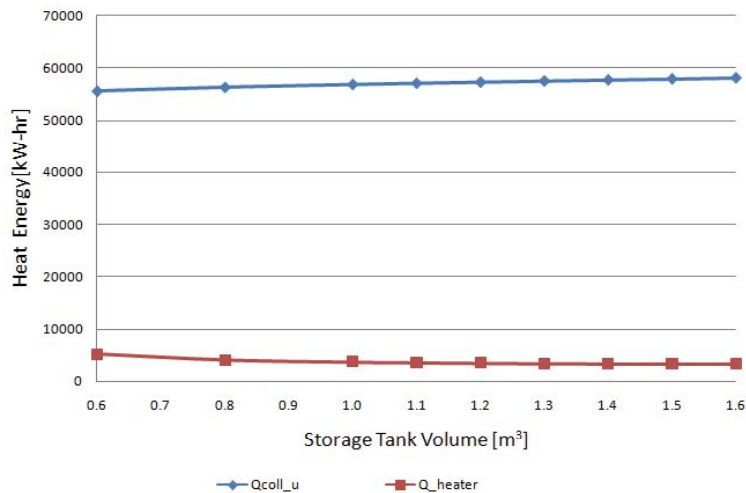


Figure 7. The influence of various storage tank sizes.

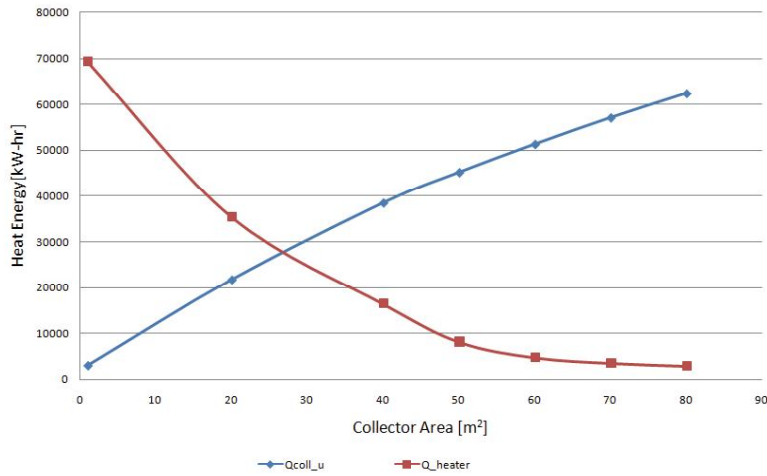


Figure 8. Collector area variation effects.

5. Overall System Behavior

The final system specifications based on the optimization study are shown in Table 5.

The energy supplied by the solar sub-system is compared to the total cooling demand of the conditioned space. The conditioned space cooling requirements include both the sensible and the latent loads.

Table 5. Final system main specifications.

Component	Parameter	Value
Collectors	Slope	12°
	Area	60 m ²
	Mass flow rate	300 kg/hr
Storage tank	Volume	1 m ³
Heater	Thermostat setting	85°C

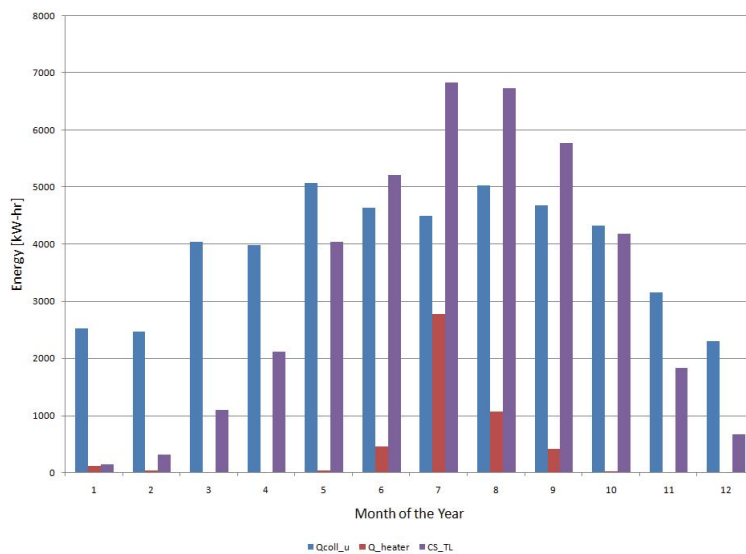


Figure 9: Monthly integrated values of the energy supplied and required.

The collector useful heat gain outside the cooling season could be utilized for domestic hot water production. The collector heat gain follows the same pattern as the total solar irradiance on tilted surface. It has been found that a large portion of the conditioned space's load is due to latent load which is dominated by the ventilation requirements. Beside the infiltration flow rate of 75 kg/hr, ACH in the range of 0.35 to 1 has been investigated in this study. For ACH of 0.5, the contribution of the latent load can be seen in Figure 10. The amount of cooling provided by the absorption cycle is higher than the sensible load. The results show that the latent load is higher during the summer where the ambient temperature is higher hence its capability to hold moisture is higher.

Moreover, the system performance has been compared to a vapor compression cycle with a COP value of 3 as shown in

Figure 11. The two systems are compared based on the required electrical energy input to provide the same cooling capacity. The results show clearly that the solar absorption cycle is feasible and it consumes less total energy per year than the VCC.

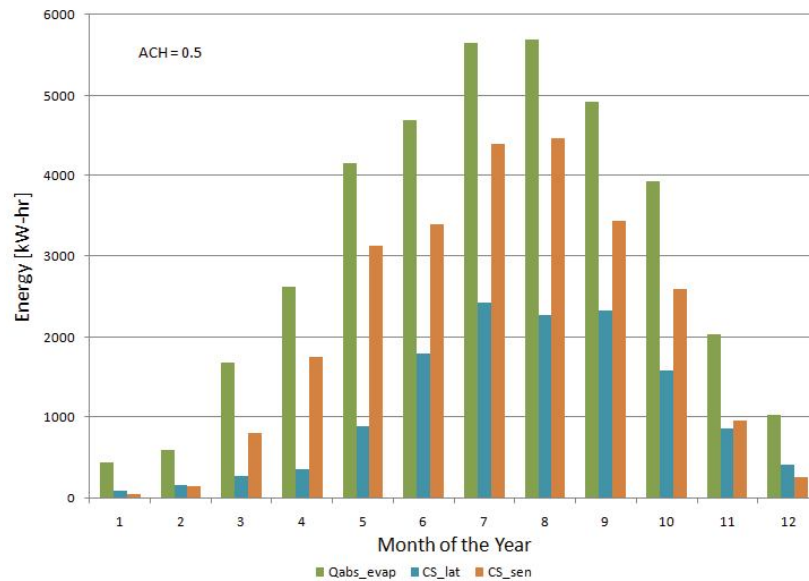


Figure 10. Conditioned space cooling loads.

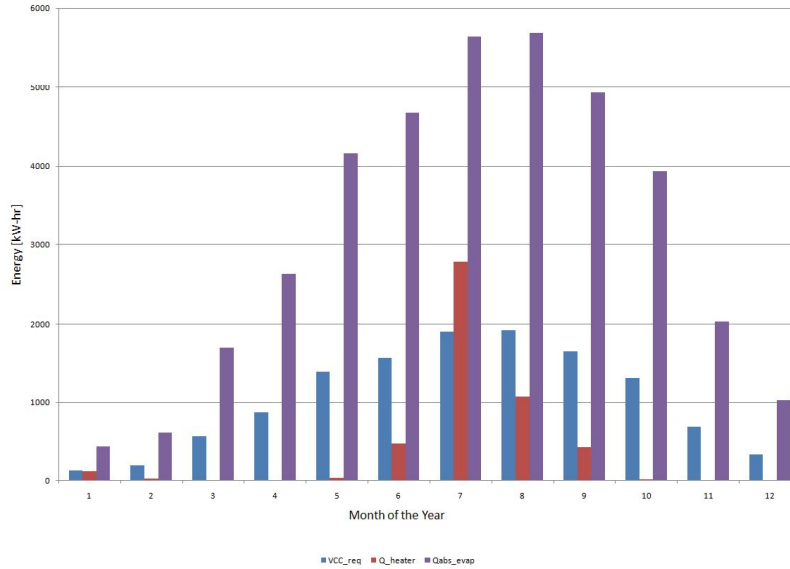


Figure 11. VCC performance vs. the solar absorption system.

6. Conclusions

The feasibility of solar driven absorption cycle has been investigated in this study. The performance of the proposed system has been optimized and sizes of different components have been determined. The results are promising and show that such system is suitable for Abu Dhabi’s weather conditions. Utilizing solar energy driven absorption air conditioners would help minimize fossil fuel-based energy use. There is a reduction in the total annual electricity consumption by 60% compared to a VCC in order to provide the same cooling effect. It would also reduce the peak electrical load on the national grid during summer. The simulation is going to be followed by an experimental work to verify the model results and determine the actual performance of the system under actual climate conditions.

Nomenclature

Symbol	Description	Unit
ACH	Air Change per Hour	1/hr
ETC	Evacuated Tube Collector	-
COP	Coefficient of Performance	-
CS	Condition Space	-
HX	Heat Exchanger	-
TMY2	Typical Meteorological Year 2	-
TRNSYS	Transient Systems Simulation	-
SACE	Solar Air Conditioning in Europe	-
SF	Solar Fraction	-
UAE	United Arab Emirates	-
VCC	Vapor Compression Cycle	-
PV	Photovoltaic	-
Parameters:		
T	Temperature	°C
m*	Mass flow rate	kg/hr
α	Absorptivity	-
ε	Emissivity	-
τ	Transmissivity	-
θ _i	Incidence angle	degrees
K	Incidence angle modifier	-
a ₀	Intercept of the collector efficiency	-
a ₁	The first-order coefficient in collector efficiency equation	W/m ² .K
a ₂	The second-order coefficient in collector efficiency equation	W/m ² .K ²
Q	Heat energy	kW-hr

P	Electrical energy	kW-hr
η	Efficiency	-
G	Total solar irradiance	W/m ²
W	Humidity ratio	kg _w /kg _a
Subscripts:		
evap	Evaporator	-
gen	Generator	-
T	Transverse	-
L	Longitude	-
coll_u	Collector useful heat gain	-
heater	Auxiliary heater	-
TL	Total load	-
elec	Electrical	-
th	Thermal	-
avg	Average	-
abs_evap	Absorption cycle's evaporator	-
lat	Latent	-
sen	Sensible	-
req	Electrical energy required	-

References

1. Al-Iriani, M.A., "Climate-related electricity demand-side management in oil exporting countries: the case of the United Arab Emirates," *Energy Policy*, Vol. 33, (2005), pp. 2350-2360.
2. Alnaser, W.E. *et al* , "Solar Energy Technology in the Middle East and North Africa (MENA) for Sustainable Energy, Water and Environment," *Advances in Solar Energy*, Vol. 17, (2007), p. 261
3. Grossman, G., "Solar-powered systems for cooling, dehumidification and air-conditioning," *Solar Energy* Vol. 72, (2002), pp. 53–62.
4. Kreith, F. and Kreider, J.F., *Principles of solar engineering*, Hemisphere publishing corporation (Washington, 1978), p. 493.
5. Osman, M. G., "Performance Analysis of a Solar Air-conditioned Villa in the Arabian Gulf," *Energy Conversion and Management*, Vol. 25, No. 3, (1985), pp. 283-293.
6. Al-Homoud, A. *et al* , "Experiences with solar cooling systems in Kuwait," *WREC-IV World Renewable Energy Congress N°4*, Denver, Colorado, Vol. 9, (1996), pp. 664-669.
7. Fathalah K. and Aly, S.E., "Theoretical Study of a Solar Powered Absorption/MED Combined System," *Energy Conversion and Management*, Vol. 31, No. 6, (1991), pp. 529-544.
8. Joudi, K.A. and Abdul-Ghafour, Q.J., "Development of design charts for solar cooling systems. Part I: computer simulation for a solar cooling system and development of solar cooling design charts," *Energy Conversion and Management* Vol. 44, (2003), pp. 313–339
9. Klein *et al*. TRNSYS 16, A transient simulation program, Solar Energy Laboratory, Madison (USA, 2007).
10. Aboulnaga, M. M., "A Roof Solar Chimney Assisted by Cooling Cavity for Natural Ventilation in Buildings in Hot Acid Climates: An Energy Conservation Approach in Al-Ain City," *Renewable Energy*, Vol. 14, (1998), pp. 357-363.
11. AboulNaga, M.M. and Abdrabboh, S.N., "Improving night ventilation into low-rise buildings in hot-arid climates exploring a combined wall-roof solar chimney," *Renewable Energy* Vol. 19, (2000), pp. 47-54.
12. Action Psychrometrics Software. Sunshine Technology, USA, 1995.
13. P.A. Davies, "A solar cooling system for greenhouse food production in hot climates," *Solar Energy*, (2005), Vol. 79, pp. 661–668.
14. Sharaf, A.M. *et al* , "Building-integrated solar photovoltaic systems - a hybrid solar cooled ventilation technique for hot climate applications," *Renewable Energy* Vol. 19, (2000), pp. 91-96.
15. El-Nashar, A. and Samad, M., "The Solar Desalination Plant in Abu Dhabi: 13 Years of Performance and Operation History," *Renewable Energy*, Vol. 14, (1998), pp. 263-274.
16. El-Nashar, A., "Effect of dust deposition on the performance of a solar desalination plant operating in an arid desert area," *Solar Energy*, Vol. 75, (2003), pp. 421–431.
17. Silicon Solar Inc, "SunMaxx Evacuated Tube Solar Collectors Technical and Installation Manual," (2008).
18. SolarNext AG, "Operating instructions / Installation manual," (2007)
19. METEONORM, "Global Meteorological Database for Engineers, Planners and Education," (2007)
20. ASHRAE. "2001 ASHRAE Fundamentals Handbook: Heating, Ventilating, and Air-Conditioning Applications," American Society of Heating, Refrigeration and Air Conditioning Engineering, Inc., (USA, 2001), CH.27.
21. McQuiston, F. *et al*, *Heating, Ventilating, and Air Conditioning Analysis and Design*, John Wiley & Sons Ltd, (USA, 2005), pp. 478.
22. Goswami, Y. *et al* , "Principles of Solar Engineering," Taylor and Francis, PA (USA, 2000), p. 234.
23. Sace, "Solar Air Conditioning in Europe," *Delft University of Technology*, (2003) NNE5/2001/25.

Author Biographies

Mr. Ali Al-Alili is currently pursuing his Ph.D. degree at the University of Maryland, U.S.A. He worked as a research assistant at the Petroleum Institute (2006-2007) after his graduation from Arizona State University (2006). His research interests are focused on solar powered cooling processes.

Dr. Didarul Islam has recently joined the Petroleum Institute as a Research Associate with extensive knowledge on heat transfer engineering. He received his Ph.D. in materials, structural and energy engineering from the University of the Ryukyus of Okinawa. Dr. Islam worked more than nine years as a lecturer and Assistant Professor in the Department of Mechanical Engineering, Rajshahi University of Engineering and Technology, Bangladesh. He has extensive teaching experience on advanced heat and mass transfer, refrigeration and air conditioning, solid mechanics and renewable energy.

Dr. Isoroku Kubo is an Associate Professor at the Petroleum Institute. He is an expert in energy conversion, heat transfer and fluid flow and an internationally recognized authority for his work on solar energy-driven power generation. Dr. Kubo has many years of industrial experience in the areas of diesel engine research and development, solar energy system development as well as management and general product development. In 2001, he joined McNeese State University (MSU) in the U.S. before coming to The Petroleum Institute in December 2004. Dr. Kubo holds a MBA degree from Indiana University, in addition to his Ph.D. in mechanical and aerospace engineering from Cornell University.

Dr. Yunho Hwang is a Research Associate Professor in the Department of Mechanical Engineering at the University of Maryland, U.S.A. His research focuses on developing comprehensive information for the detailed physics of transport processes, new cost-effective test methods, and innovative components and systems. He is responsible for the Alternative Cooling Technologies and Applications Consortium (ACTA) that is sponsored by industry, government and research institutions.

Dr. Reinhard Radermacher is a Professor in the Department of Mechanical Engineering at the University of Maryland, U.S.A. He holds a M.S. and Ph.D. in Physics from the Munich Institute of Technology. Dr. Radermacher is an internationally recognized expert in heat transfer and working fluids for energy conversion systems, including heat pumps, air-conditioners, and refrigeration systems.